



## NRC Publications Archive Archives des publications du CNRC

### Observation of hole burning and cross relaxation effects in ruby Szabo, A.

This publication could be one of several versions: author's original, accepted manuscript or the publisher's version. / La version de cette publication peut être l'une des suivantes : la version prépublication de l'auteur, la version acceptée du manuscrit ou la version de l'éditeur.

For the publisher's version, please access the DOI link below. / Pour consulter la version de l'éditeur, utilisez le lien DOI ci-dessous.

#### **Publisher's version / Version de l'éditeur:**

<https://doi.org/10.1103/PhysRevB.11.4512>

*Physical Review B*, 11, 11, pp. 4512-4517, 1975-06

#### **NRC Publications Record / Notice d'Archives des publications de CNRC:**

<https://nrc-publications.canada.ca/eng/view/object/?id=b39fa4be-fc4f-48c5-b2c0-5a1aac8967be>

<https://publications-cnrc.canada.ca/fra/voir/objet/?id=b39fa4be-fc4f-48c5-b2c0-5a1aac8967be>

Access and use of this website and the material on it are subject to the Terms and Conditions set forth at

<https://nrc-publications.canada.ca/eng/copyright>

READ THESE TERMS AND CONDITIONS CAREFULLY BEFORE USING THIS WEBSITE.

L'accès à ce site Web et l'utilisation de son contenu sont assujettis aux conditions présentées dans le site

<https://publications-cnrc.canada.ca/fra/droits>

LISEZ CES CONDITIONS ATTENTIVEMENT AVANT D'UTILISER CE SITE WEB.

**Questions?** Contact the NRC Publications Archive team at

PublicationsArchive-ArchivesPublications@nrc-cnrc.gc.ca. If you wish to email the authors directly, please see the first page of the publication for their contact information.

**Vous avez des questions?** Nous pouvons vous aider. Pour communiquer directement avec un auteur, consultez la première page de la revue dans laquelle son article a été publié afin de trouver ses coordonnées. Si vous n'arrivez pas à les repérer, communiquez avec nous à PublicationsArchive-ArchivesPublications@nrc-cnrc.gc.ca.



## Observation of hole burning and cross relaxation effects in ruby

A. Szabo

*Radio and Electrical Engineering Division, National Research Council of Canada, Ottawa, Ontario K1A 0R8*

(Received 1 July 1974)

In this paper we report, for the first time, the observation of optical hole burning in a solid, ruby. In addition, we describe experimental results which show that optical saturation of the inhomogeneously broadened  $R_1$  line in ruby at 4.2°K occurs not only for ions in resonance with the saturating radiation but also for ions at frequencies up to about 50 MHz away from the radiation frequency. This result and others are consistent with a model in which cross relaxation occurs in the ground-state levels between ions in resonance with the laser beam and nonresonant ions.

### INTRODUCTION

In the past eight years, several new laser techniques have been developed which allow spectroscopy whose resolution is limited only by the homogeneous linewidth for gaseous and solid-state inhomogeneously broadened spectra. The techniques parallel conventional types of spectroscopy in that line-narrowing phenomena are observed both in absorption and fluorescence. Absorption hole burning was first observed in gases<sup>1</sup> using the Lamb-dip effect and is presently giving unparalleled resolution in gaseous spectroscopy.<sup>2</sup> Fluorescence line narrowing (FLN) in gases was first<sup>3</sup> observed via excited-state-coupled transitions in Ne and later<sup>4</sup> in  $I_2$  following excitation from the ground state. FLN has also been extended to solids.<sup>5</sup> In this paper we would like to report on a new technique of hole-burning spectroscopy and the application of this technique in the first direct observation of optical hole burning in a solid (ruby). While such an observation in ruby is not unexpected in view of the FLN experiments,<sup>5</sup> new effects appear which are shown to be associated with ground-state cross relaxation.

### EXPERIMENTAL

The radiation source used in the experiments was a tunable single-frequency cw ruby laser.<sup>5,6</sup> By varying the temperature of the laser ruby, the laser frequency could be tuned continuously over a range of several GHz. The tuning capability is illustrated in Fig. 1, which shows the ruby absorption spectrum in the vicinity of the  $\bar{E} \rightarrow {}^4A_2(\pm \frac{1}{2})$  line [ $R(\pm \frac{1}{2})$ ]. The well-known isotope structure is shown with much higher resolution than previous work<sup>7</sup> and a precise demonstration of the Gaussian line shape is given. In the hole-burning experiments, the laser frequency was adjusted to the peak ( $\pm 50$  MHz) of the  $R(\pm \frac{1}{2})$  line.

Since the Lamb-dip effect used for hole-burning spectroscopy in gases is, of course, not applicable to a solid, another approach is required. For an inhomogeneously broadened line in a solid, two

laser sources are required for hole-burning spectroscopy: a fixed saturating beam to produce the hole and a tunable low-power beam to probe the absorption in the vicinity of the hole. A simple way to produce such beams is to weakly amplitude modulate a single-frequency laser. The sidebands then serve as the probe while the carrier serves as the saturating beam. Measurement of the sideband beam transmission through the sample as a function of modulation frequency gives the hole shape produced by the saturating carrier.

The experimental arrangement is shown in Fig. 2. The laser beam first passes through a Coherent Associates model 3025 electro-optic modulator which has a bandwidth of 25 MHz. The modulation amplitude is adjusted so that the sideband power is sufficiently low so as to be nonsaturating. The beam is then focused by a 10-cm lens into the ruby sample which is cooled to  $\sim 5$ °K. The transmitted beam is detected by an RCA 31000 A photomultiplier; the output of which is processed by a Hewlett Packard model 8553B, 8552B, 141T spectrum analyzer. The sideband intensity is obtained by superheterodyne detection with the transmitted carrier beam serving as the local oscillator. The system is calibrated versus modulation frequency by removing the ruby sample and adjusting the photomultiplier-local-oscillator current (by attenuating the beam) to be the same as with the sample in position.

### RESULTS AND DISCUSSION

#### Hole burning

The experimental dependence of the transmitted sideband intensity on modulation frequency is shown in Fig. 3. Two main features of these results are (i) the hole width for zero magnetic field is much larger than when there is an applied field (narrow central line) and (ii) for the applied field case, there are two holes of half-widths  $\sim 5$  and  $\sim 50$  MHz.

The observed narrowing of the homogeneous linewidth in a magnetic field agrees with photon

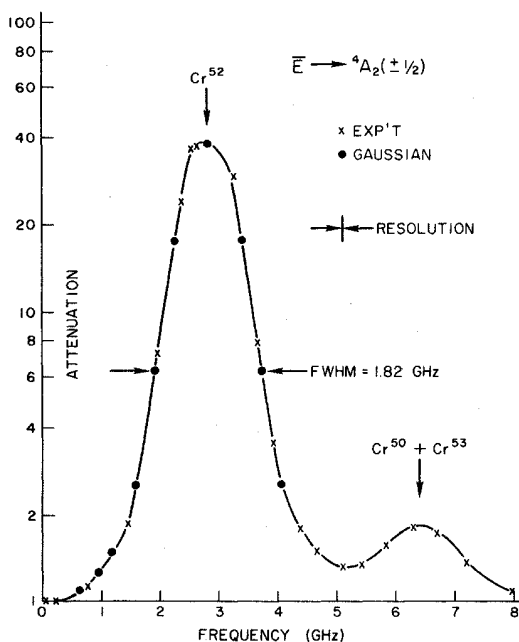


FIG. 1. Absorption spectrum near the  $R_1(\pm\frac{1}{2})$  line of 0.03% ruby at 4.2°K using a tunable single-frequency ruby laser.

echo<sup>8</sup> and fluorescence-line-narrowing<sup>5</sup> results. Magnetic-field-dependence studies<sup>8,9</sup> of photon echoes indicate an echo lifetime lengthening of over an order of magnitude when the magnetic field is turned on, which is consistent with a reduction of the homogeneous linewidth. In FLN studies a linewidth of 120 MHz has been observed for a 0.01% ruby in zero field and an instrument-limited width of 9 MHz for an applied field.<sup>10</sup> The reduction of the homogeneous linewidth with magnetic field may be understood in terms of a simple classical picture. At zero applied field, an isotropic fluctuating magnetic field exists at the Cr sites due to the Al nuclear spins. This magnetic field produces a modulated splitting of the energy levels giving rise to a linewidth. When a magnetic field, large compared with the Al field, is applied along the  $c$  axis, the total field remains mainly oriented along the  $c$  axis with a small

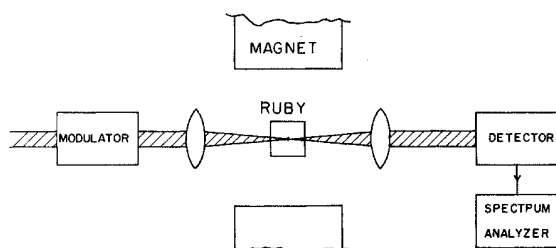


FIG. 2. Schematic of apparatus used for sideband detection of hole burning.

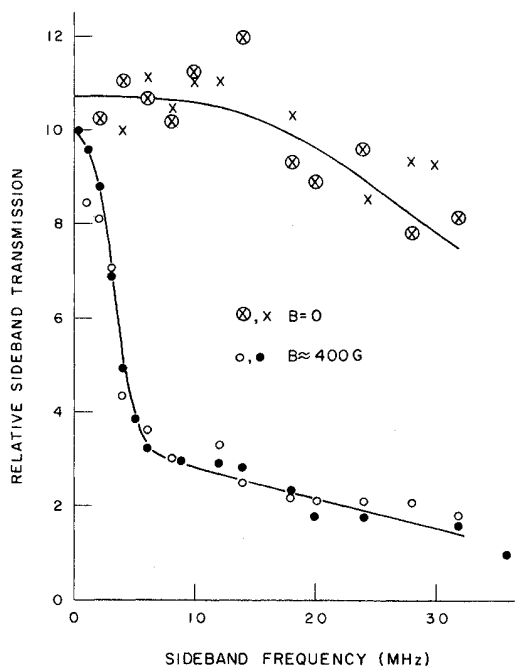


FIG. 3. Dependence of sideband-transmitted intensity on frequency shift from the saturating carrier.

modulation of its amplitude present owing to the Al spins. Since the Zeeman splitting of the  $R_1(\pm\frac{1}{2})$  line is least when the field is along the  $c$  axis, a reduction in linewidth occurs.

The observed linewidth of 5 MHz for an applied magnetic field is mainly determined by the laser linewidth, the latter being determined by pump-power fluctuations and vibrations.<sup>6</sup> The homogeneous linewidth is expected to be determined by Al-Cr superhyperfine interactions.<sup>5</sup> Calculations based on recent<sup>11</sup> measurements of the superhyperfine interaction constants in the excited  $\bar{E}$  states give a linewidth for  $R(\pm\frac{1}{2})$  transitions of 0.54 MHz. Another calculation based on fluorescence-decay considerations has predicted<sup>12</sup> linewidths in the range 0.7–0.9 MHz.

#### Cross relaxation

Of particular interest is the fact that two holes appear for an applied magnetic field. At first sight, this result seems to suggest that optical cross relaxation leading to spectral diffusion occurs. However, we argue that optical cross relaxation is not the mechanism for spectral diffusion but instead it is cross relaxation in the ground-state levels. A simple and direct proof that optical cross relaxation does not occur is that in FLN experiments, there is no evidence of a broad fluorescence line sitting under a narrow one.

Further evidence favoring ground-state cross relaxation is given in Fig. 4, which shows the cw

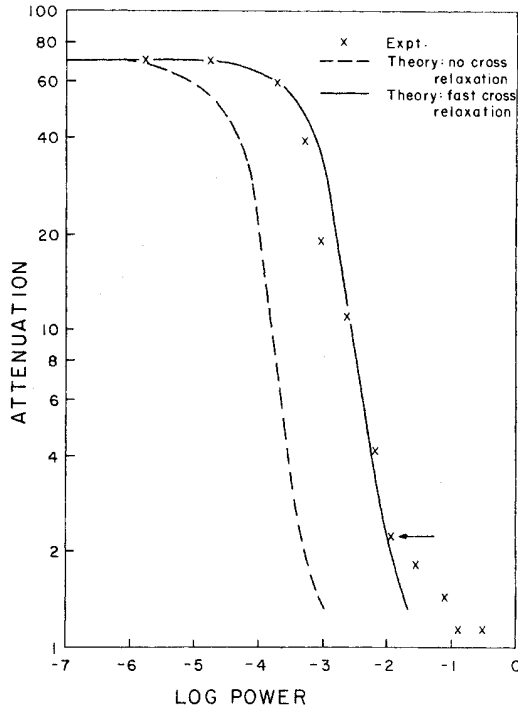


FIG. 4. Optical saturation behavior of 0.03% ruby at 4.2°K using a 10-cm focusing lens. On the horizontal axis, zero corresponds to 1 mW of laser power. The laser is tuned to the center of the  $R_1(\pm \frac{1}{2})$  line and 400-G field is applied along the  $c$  axis. The arrow shows power at which Fig. 3 was obtained.

saturation behavior of ruby. We have compared experimental results with calculations described in the Appendix. The saturation is observed to agree well with the theory in which fast cross relaxation is assumed. The only adjustable parameter in Eq. (A4) is  $\sigma_h$ , the effective homogeneous cross section which, in the present experiment, is determined by the laser linewidth. The pump photon density is determined by the input-beam diameter of 2 mm and the 10-cm focusing lens. Direct Fabry-Perot and superheterodyne measurements using two separate lasers place an upper limit of 5 MHz on the laser linewidth.<sup>6</sup> To shift the no-cross-relaxation curve onto the experimental results would require a laser linewidth of about 100 MHz which is far from the actual value. Hence we conclude that fast cross relaxation is present.

A rate-equation analysis of cross relaxation will now be presented. We divide the ions into three classes, the R ions resonant with the laser, the NR ions which are near resonance, and the NR ions which are far off resonance. The analysis and qualitative study of Fig. 5 show how cross relaxation to NR ions can lead to a reduction of optical absorption and hence the production of a hole

by NR ions. The experimental results of Fig. 3 suggest that only R and NR ions are involved in the cross relaxation. If all ions were involved in the cross relaxation, it is easy to show that very little redistribution of ground-state population of the unpumped ions would occur essentially because the number of unpumped ions is so much greater than the pumped ones (by a factor  $\sim 400$ ). In order to get an appreciable redistribution of population of the unpumped ions due to cross relaxation from the pumped ones, it is necessary to restrict the number of the former. It is interesting to note that since cross relaxation occurs preferentially amongst ions which are closest, the experiment suggests that the frequency of the ions changes gradually from site to site rather than suddenly, in other words the strain responsible for the inhomogeneous broadening is of macroscopic size compared with the ion spacing.

To make the problem tractable we simplify the six-level ruby system (two optical, four microwave in a magnetic field) to three levels. For the energy-level scheme shown in Fig. 5, levels 1 and 2 are ground-state levels with a microwave-frequency separation while 3 is an optical level. The optical transitions 1-3, 2-3 are inhomogeneously broadened. A saturating single-frequency laser beam interacts with transition 2-3. We will assume ground-state cross relaxation can occur only between R and NR ions.

The rate equation for R ions in level 1 may be written

$$\frac{dn_1}{dt} = -\beta(n_1 - n_2) + \gamma n_3 - (\omega/N)(n_1 N_2 - n_2 N_1), \quad (1)$$

where  $\beta = 5 \text{ sec}^{-1}$  is the spin-lattice relaxation rate at 4°K,  $\gamma = 250 \text{ sec}^{-1}$  is the  $\bar{E}$ -level relaxation rate, and  $\omega \approx 10^6 \text{ sec}^{-1}$  is the cross-relaxation rate for pink ruby.<sup>13</sup> The density of NR ions is denoted by  $N$  and similarly  $n$  for R ions. The rate equation for NR ions in level 2 is

$$\frac{dN_2}{dt} = -\beta(N_2 - N_1) - (\omega/N)(n_1 N_2 - n_2 N_1). \quad (2)$$

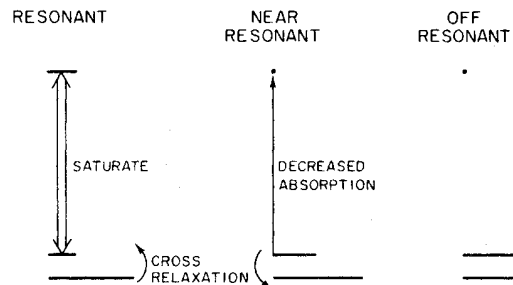


FIG. 5. Energy-level scheme for cross-relaxation model.

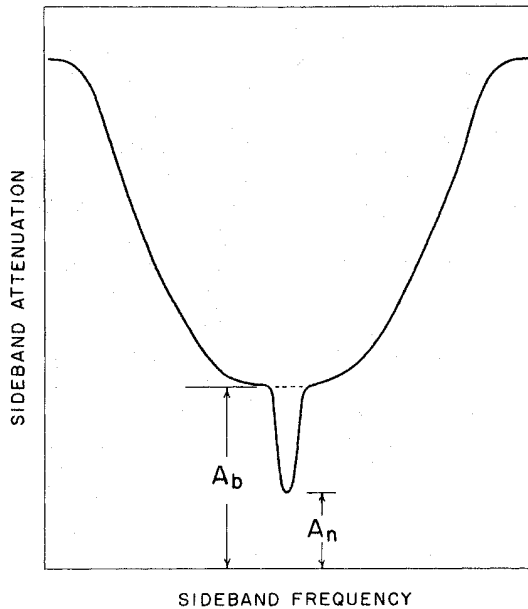


FIG. 6. Absorption hole shape as seen by the probe sideband beam in the vicinity of the saturating line.  $A_n$  is the probe attenuation at the saturating line position and  $A_b$  is the probe attenuation extrapolated to the center of the broad hole.

Solving (1) and (2) under steady-state conditions and with strong pumping (i. e.,  $n_2 = n_3$ ), we obtain an equation for  $N_2$ :

$$2\omega\beta N_2^2 + [\omega\beta(N+2n) + 6\beta^2 N + \gamma(\omega n + 2\beta N)]N_2 - \beta N[\omega(N+n) + (3\beta + \gamma)N] = 0. \quad (3)$$

For  $n/N \ll 1$  and  $\omega \gg \beta, \gamma$  we may approximate Eq. (3) as

$$2\beta N_2^2 + (N\beta + \gamma n)N_2 - \beta N^2 = 0, \quad (4)$$

which has for its solution

$$N_2/N = \frac{1}{2} \left[ -(1+x) + (9+2x+x^2)^{1/2} \right], \quad (5)$$

where  $x = \gamma n/\beta N = 50n/N$ . We note that  $\omega$  drops out of the above equation, essentially because it is much larger than the other relaxation rates. Physically this means that the ground-state spin temperature of the NR ions is locked to that of the R ions. Measurement of  $N_2/N$  then allows calculation of the ratio  $n/N$  and hence the holewidth of  $N$  corresponding to the NR ions.

From Fig. 4, we obtain for the differential attenuation  $A_n$  at the operating point indicated  $A_n = 1.3$ . This is the attenuation seen by the sideband probe at the peak of the narrow line in Fig. 3. The sideband attenuation  $A_b$  produced by the broad line extrapolated to the center of the broad line is, from Fig. 3, about a factor of 2.5 larger or  $A_b = 3.2$ . The various attenuations are shown in Fig. 6. Referring to Fig. 5, the population  $N_2$  in level 2 of

NR ions in the broad hole is given by  $A_b = e^{\sigma_b N_2 l}$ , where  $\sigma_b$  is a cross section determined by  $\sigma_b N = \sigma_i N_T$ , where  $N$  is the population density of NR ions,  $\sigma_i$  is the inhomogeneous cross section, and  $N_T$  is the total density of Cr ions. Hence we obtain  $N_2/N = \ln A_b / \sigma_i N_T l$ . The measurement in Fig. 1 gives  $\sigma_i = 2.56 \times 10^{-18} \text{ cm}^2$  giving  $N_2/N = 0.16$  for  $l = 3 \text{ mm}$  and a Cr density  $N_T = 0.96 \times 10^{19} / \text{cm}^3$ .

From Eq. (5) we obtain  $x = 50n/N = 5.0$  and therefore  $n/N = \frac{1}{10}$ . Taking a 5 MHz width for  $n$  (determined by the laser linewidth) gives a width of 50 MHz for  $N$  in good agreement with the experimental broad-hole width. Thus we have shown that the observed attenuation in the broad hole is consistent with the hole width using a model in which cross relaxation is restricted between resonant and near-resonant ions.

#### Further evidence for cross relaxation

Here we present further evidence that cross relaxation occurs in the ground-state levels. The evidence involves time-dependent absorption and fluorescence processes. In Fig. 7 we show the time dependence of the transmission after suddenly turning the saturating light on and in Fig. 8 the absorption recovery after suddenly reducing the light from a high saturating level to a low monitoring level. While not of direct interest here, Fig. 7 shows rather nicely the effect of a magnetic field on the saturation behavior via its effect on the homogeneous linewidth [Eq. (A4) in the Appendix]. Much less saturation is observed for zero field because of the larger homogeneous linewidth in zero field. The absorption recovery in Fig. 8 is seen

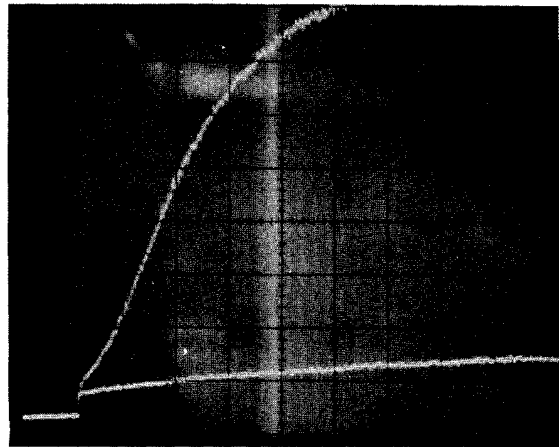


FIG. 7. Time dependence of transmission (transmission increasing upwards) for  $R(\pm \frac{1}{2})$  line when the saturating radiation is suddenly turned on. A magnetic field of  $\sim 400 \text{ G}$  is applied parallel to the  $c$  axis for the large-amplitude trace. The field is zero for the small-amplitude trace. Time scale 1 msec/division.

to occur predominately at a fast msec rate followed by a smaller-amplitude 0.2 sec rate, which corresponds to the ground-state relaxation time. If there were no cross relaxation we would have expected to see a recovery mainly at a 0.2 sec rate because of optical-pumping effects in the ground state. In Fig. 9 we show the time dependence of the fluorescence following a sudden application of a saturating pulse. The fluorescence of the  $R_1(\pm\frac{3}{2})$  transition was observed using a Fabry-Perot interferometer,<sup>5</sup> which allowed discrimination against scattered laser light which excited the  $R_1(\pm\frac{1}{2})$  transition. If there were no cross relaxation we would expect a sudden increase in fluorescence corresponding to a sudden increase of population of  $\frac{1}{4}N_T$  in  $\bar{E}$  followed by a drop to a level corresponding to a population  $\sim(\beta/\gamma)N_T = \frac{1}{50}N_T$  in  $\bar{E}$ , the latter drop occurring because of optical pumping in the ground state. Experimentally less than a factor of 2 drop in fluorescence is observed, much less than the factor  $\frac{50}{4}$  expected from the above argument. The fact that some drop occurs indicates some restriction in the population between which cross relaxation occurs which is consistent with earlier conclusions. If fast cross relaxation occurred to the entire population a slight rise rather than a drop in fluorescence would be expected as the excited-state population increases from its turn-on value  $\frac{1}{4}N_T$  to  $\frac{1}{3}N_T$ , the value reached when the ground-state populations are constrained to be equal because of cross relaxation.

#### CONCLUSION

The main conclusions of this study are:

- (i) Optical hole burning has been observed for the first time in a solid.
- (ii) A decrease in hole width corresponding to a

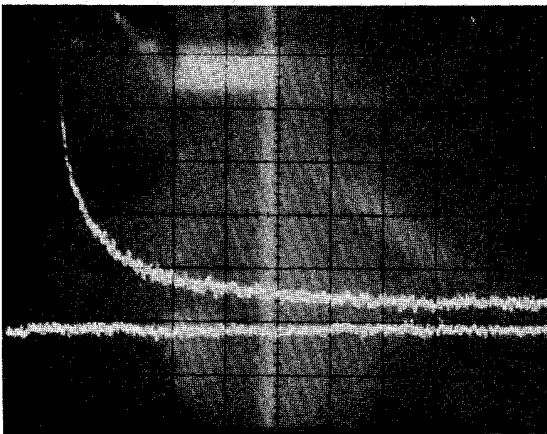


FIG. 8. Recovery of absorption following saturation. The bottom trace shows the final recovered value. Time scale 2 msec/cm. 400-G field applied along  $c$  axis.

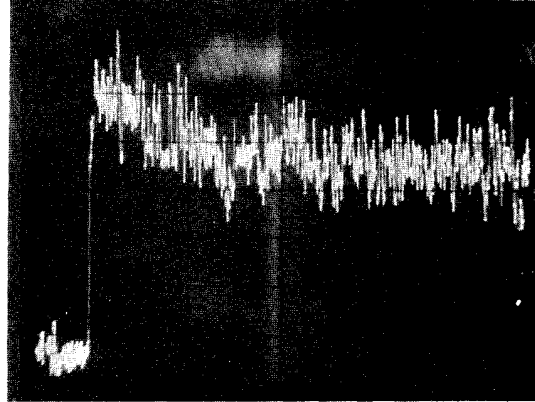


FIG. 9. Time dependence of  $R_1(\pm\frac{3}{2})$  fluorescence on suddenly turning on laser to excite  $R_1(\pm\frac{1}{2})$  line. Time scale 0.1 sec/cm. Zero applied field.

decrease in the homogeneous linewidth occurs when a magnetic field is applied to the ruby sample. This is in agreement with fluorescence-line-narrowing<sup>5</sup> and photon-echo<sup>8</sup> results.

(iii) In a magnetic field the narrow hole is superimposed on a much broader hole. The broad hole arises from cross relaxation in the ground-state levels between optically resonant ions and near-resonant ions.

(iv) The strain causing inhomogeneous broadening of the R zero-phonon line in ruby varies slowly spatially compared with the ion spacing.

(v) Higher-resolution spectroscopy is expected for hole burning as compared with fluorescence line narrowing since an interferometer with its limited resolution is not required. The resolution is determined only by the laser stability.

#### ACKNOWLEDGMENTS

Discussions with Dr. L. E. Erickson and the technical assistance of E. L. Dimock are gratefully acknowledged.

#### APPENDIX: OPTICAL TRANSMISSION UNDER SATURATION CONDITIONS

We consider transmission under saturation conditions for the three-level system shown in Fig. 5. The population and photon rate equations are, ignoring cross relaxation,

$$\frac{dn_1}{dt} = \beta(n_2 - n_1) + \gamma n_3, \quad (\text{A1})$$

$$\frac{dn_2}{dt} = \sigma_h P(n_3 - n_2) + \gamma n_3 - \beta(n_2 - n_1), \quad (\text{A2})$$

and

$$\frac{dP}{dx} = \sigma_h P(n_3 - n_2), \quad (\text{A3})$$

where  $\sigma_h$  is the cross section corresponding to the

homogeneous linewidth and  $P$  is the photon flux. The solution of Eqs. (A1)–(A3) under steady-state conditions is

$$\left(\frac{3\beta+\gamma}{4\beta\gamma}\right)\sigma_h(P-P_0)+\ln P/P_0=-\frac{1}{2}\sigma_i N_T l, \quad (\text{A4})$$

where  $\sigma_i$  is the inhomogeneous cross section,  $N_T$  is the total population,  $P_0$  is the incident photon flux, and  $l$  is the sample length.

In the case of fast cross relaxation to a reser-

voir of atoms much larger in number than the resonant atoms, it may be shown by considering cross-relaxation terms in Eqs. (A1) and (A2) that Eq. (A4) becomes approximately,

$$(3/4\gamma)\sigma_h(P-P_0)+\ln P/P_0=-\frac{1}{2}\sigma_i N_T l. \quad (\text{A5})$$

This agrees with intuitive arguments in which we let an effective  $\beta$  become very large since the real one is short circuited by fast cross relaxation.

<sup>1</sup>P. H. Lee and M. L. Skolnick, *Appl. Phys. Lett.* **10**, 303 (1967).

<sup>2</sup>J. L. Hall and C. Bord e, *Phys. Rev. Lett.* **30**, 1101 (1973).

<sup>3</sup>W. G. Schweitzer, Jr., M. M. Birky, and J. A. White, *J. Opt. Soc. Amer.* **57**, 1226 (1967).

<sup>4</sup>A. Szabo and L. E. Erickson, *Opt. Commun.* **5**, 287 (1972).

<sup>5</sup>A. Szabo, *Phys. Rev. Lett.* **25**, 924 (1970); **27**, 323 (1971).

<sup>6</sup>A. Szabo, *J. Appl. Phys.* (to be published).

<sup>7</sup>G. F. Imbusch, W. M. Yen, A. L. Schawlow, G. E. Devlin, and J. P. Remeika, *Phys. Rev.* **136**, A481 (1964).

<sup>8</sup>N. A. Kurnit and S. R. Hartmann, *Interaction of Radiation with Solids* (Plenum, New York, 1967), pp. 693–701.

<sup>9</sup>P. F. Liao and S. R. Hartmann, *Opt. Commun.* **8**, 310 (1973).

<sup>10</sup>A. Szabo (unpublished work). The instrument width is determined by the Fabry-Perot width of 5 MHz and the laser linewidth of 2–5 MHz.

<sup>11</sup>P. F. Liao, P. Hu, R. Leigh, and S. R. Hartmann, *Phys. Rev. A* **9**, 332 (1974).

<sup>12</sup>L. Q. Lambert, *Phys. Rev. B* **7**, 1834 (1973).

<sup>13</sup>R. L. Kyhl and B. P. Nageswara-Rao, *Phys. Rev.* **158**, 284 (1967).

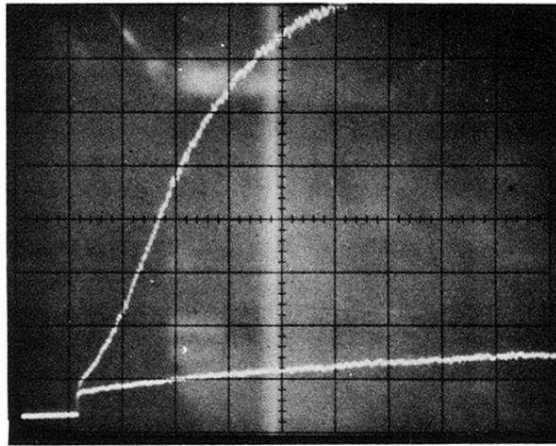


FIG. 7. Time dependence of transmission (transmission increasing upwards) for  $R(\pm \frac{1}{2})$  line when the saturating radiation is suddenly turned on. A magnetic field of  $\sim 400$  G is applied parallel to the  $c$  axis for the large-amplitude trace. The field is zero for the small-amplitude trace. Time scale 1 msec/division.



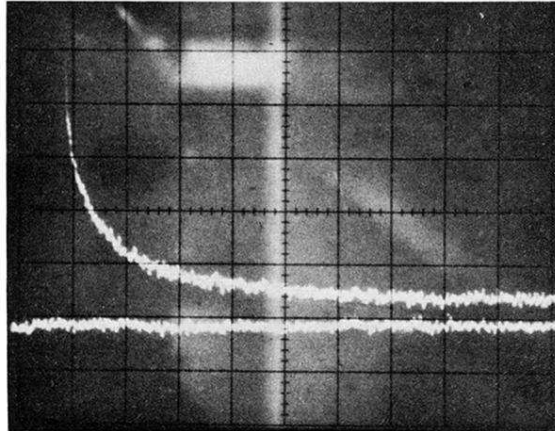


FIG. 8. Recovery of absorption following saturation. The bottom trace shows the final recovered value. Time scale 2 msec/cm. 400-G field applied along  $c$  axis.

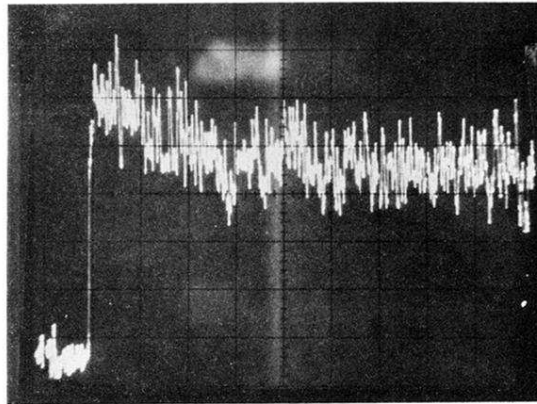


FIG. 9. Time dependence of  $R_1(\pm\frac{3}{2})$  fluorescence on suddenly turning on laser to excite  $R_1(\pm\frac{1}{2})$  line. Time scale 0.1 sec/cm. Zero applied field.